Title	**Biomineralization mediated by anaerobic methane-consuming cell consortia**
Author(s)	**Chen, Y; Li, Y; Zhou, GT; Li, H; Lin, YT; Xiao, X; Wang, FP**
Citation	**Scientific Reports, 2014, v. 4, article no. 5696**
Issued Date	**2014**
URL	**http://hdl.handle.net/10722/200596**
Rights	**Creative Commons: Attribution 3.0 Hong Kong License**

Biomineralization mediated by anaerobic methane-consuming cell consortia

Ying Chen[1,2], Yi-Liang Li[3], Gen-Tao Zhou[4], Han Li[4], Yang-Ting Lin[5], Xiang Xiao[1,2] & Feng-Ping Wang[1,2]

[1]State Key Laboratory of Microbial Metabolism, School of Life Sciences and Biotechnology, Shanghai Jiao Tong University, Shanghai 200240, People's Republic of China, [2]State Key Laboratory of Ocean Engineering, School of Naval Architecture, Ocean and Civil Engineering, Shanghai Jiao Tong University, Shanghai 200240, People's Republic of China, [3]Department of Earth Sciences, The University of Hong Kong, Hong Kong, China, [4]CAS Key Laboratory of Crust-Mantle Materials and Environments, School of Earth and Space Sciences, University of Science and Technology of China, Hefei 230026, China, [5]Key Laboratory of the Earth's Deep Interior, Institute of Geology and Geophysics, Chinese Academy of Sciences, Beijing 100029, China.

Anaerobic methanotrophic archaea (ANME) play a significant role in global carbon cycles. These organisms consume more than 90% of ocean-derived methane and influence the landscape of the seafloor by stimulating the formation of carbonates. ANME frequently form cell consortia with sulfate-reducing bacteria (SRB) of the family Deltaproteobacteria. We investigated the mechanistic link between ANME and the natural consortium by examining anaerobic oxidation of methane (AOM) metabolism and the deposition of biogenetic minerals through high-resolution imaging analysis. All of the cell consortia found in a sample of marine sediment were encrusted by a thick siliceous envelope consisting of laminated and cementing substances, whereas carbonate minerals were not found attached to cells. Beside SRB cells, other bacteria (such as Betaproteobacteria) were found to link with the consortia by adhering to the siliceous crusts. Given the properties of siliceous minerals, we hypothesize that ANME cell consortia can interact with other microorganisms and their substrates via their siliceous envelope, and this mechanism of silicon accumulation may serve in clay mineral formation in marine sedimentary environments. A mechanism for biomineralization mediated by AOM consortia was suggested based on the above observations.

Anaerobic oxidation of methane (AOM) is frequently coupled to sulfate reduction and this reaction is mediated by the association between anaerobic methanotrophic archaea (ANME) and sulfate-reducing bacteria (SRB). ANME can be divided into three phylogenetic groups, ANME-1, -2, and -3, which are related to the *Methanosarcinales* and *Methanomicrobiales* methanogens[2–6], whereas SRB mainly belong to the *Desulfosarcina/Desulfococcus* (DSS) of Deltaproteobacteria[7]. In addition, Alphaproteobacteria related to *Sphingomonas* spp. and Betaproteobacteria related to *Burkholderia* spp. have also been observed as the dominant or sole bacterial partner with ANME-2[8]. These organisms form AOM microbial consortia and are widely distributed, from marine cold seep systems, the sulfate-methane transition zone of sediments, hydrothermal vents, the deep biosphere, and marine water columns to terrestrial habitats such as mud volcanoes, landfills, and the anoxic water of freshwater lakes[1,9–13]. In some environments, the abundance of the consortia can reach a concentration of 10^7 aggregates/cm^3 of sediment[14]. However, due to the slow growth rate and long doubling time of AOM consortia, no pure ANME and/or associated SRB cells have been cultivated in the laboratory yet.

As AOM provides carbon and energy sources for the growth of ANME[15], it leads to a significant increase in alkalinity, dissolved inorganic carbon, and sulfide, which induces the precipitation of carbonates and iron sulfides[16]. This microbial process may shape the seafloor landscape by fostering the building of carbonate chimneys, nodules, and pavements[17,18]. However, the mechanistic link between the metabolism of the AOM consortia and the deposition of authigenic minerals has yet to be found.

The AOM consortia comprised of ANME-2 and SRB have diameters of around 3–20 μm, are spherical in shape, and have two different spatial arrangements of cells, shell-type and mixed-type. Shell-type consortia have a well-known morphology with an inner core of ANME, which is partially or fully surrounded by outer SRB, whereas the ANME and SRB of the mixed-type are completely mixed to form irregular shapes[1].

In addition to the various spatial arrangements of cells, it has been observed that the consortia, particularly those containing ANME-2, are enclosed by a thick organic matrix[1,19]. Given the significant roles of extracellular
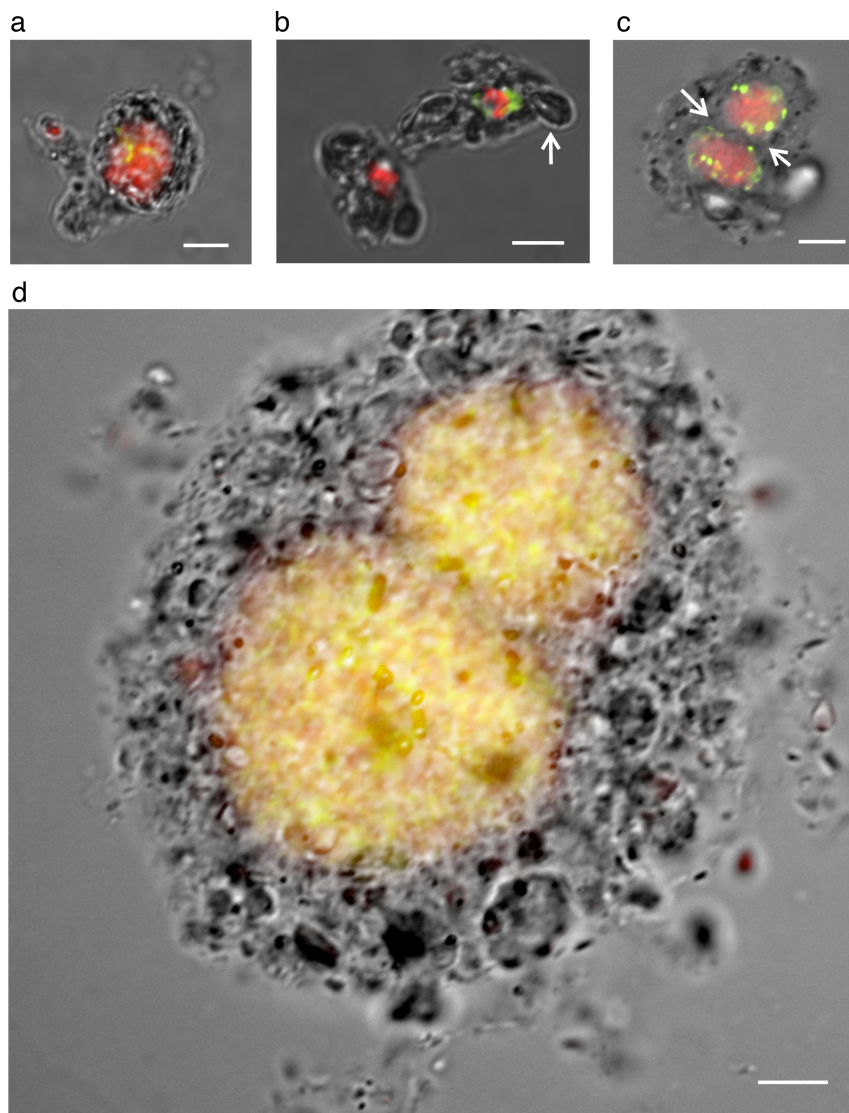
Figure 1 | Overlays of light micrographs and FISH-stained micrographs of AOM consortia from the stored marine sedimentary sample, in which the ANME are in red and the SRB are in green. Observations from stored marine sedimentary samples (a–c) and enriched culture (d): (a) a typical microbial consortium with an envelope; (b) two small consortia with a thick envelope and a sizeable deposition (arrow) associating with a cell consortium; and (c, d) fissuring AOM consortia with a consortia envelope. The arrows in (c, d) highlight the interface of the dividing consortia. In all cases, the scale bars represent 5 μm.

polymeric substances[20], the organic matrix of AOM consortia may facilitate the nucleation of minerals. However, the composition and the mechanism of mineralization on the exopolymers of the AOM of such consortia are poorly understood.

The present study was designed to understand both the mechanistic links between ANME and the associated bacterial cells and AOM metabolism involved in the deposition of biogenetic minerals. High-resolution imaging analysis combined with fluorescence *in situ* hybridization (FISH), light microscopy, scanning electron microscopy (SEM), energy-dispersive X-ray spectroscopy (EDS), and nanometer-scale secondary ion mass spectrometry (NanoSIMS) were used to delineate the biogeochemical microenvironments of AOM. Cell staining, FISH, light microscopy, and a combination of NanoSIMS/SEM techniques were used to localize and image the ion distribution of the inner layers of the consortia directly on the environmental samples without the use of ultrathin sections.

Results

Light micrographs of consortia envelopes. The sample was collected from sediment of 0–40 cm in depth that was obtained from the Capt Aryutinov mud volcano located at a depth of 1200 m in the Gulf of Cadiz. The mud mainly contained carbonates, quartz, and clay, as shown in Supplementary Figure S1–3. This sample was stored at ambient pressure in artificial seawater supplemented with methane at 4°C. Light micrographs showed that ANME-2-SRB consortia within the stored sediment sample were entirely surrounded by amassing crusts (Figure 1a–c), forming consortia envelopes, which were recognized as a thick organic matrix in previous reports[1,19]. These envelopes were consistently observed in the enriched AOM culture sample (Figure 1d), indicating their formation during cell enrichment. These extracellular structures had a thickness ranging from 0.5 to 7 μm. FISH experiments on AOM consortia showed that this structure was permeable and had limited optical transparence. Amorphous minerals were clearly observed on the envelope (Figure 1b). When the AOM consortia grew in size, they formed small aggregates of "buds" and fissures[22]. A number of consortia were captured undergoing fission within the envelope (e.g., Figure 1c, d) and a new part of the envelope was observed forming at the interface between two daughter consortia (Figure 1c, d). These observations suggested that the envelope structure might functionally
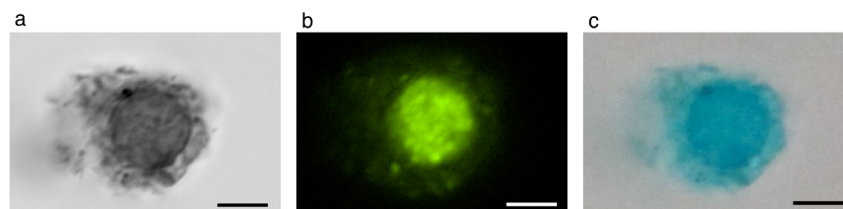
Figure 2 | **FITC and Alcian Blue staining of a consortium from the stored marine sedimentary sample, (a) without staining, (b) with FITC staining, and (c) with Alcian Blue staining. In all cases, the scale bars represent 5 μm.**

affect the physiology of the cells within the structure. Proteins and polysaccharides were detected on the envelope by the use of FITC and Alcian Blue staining, respectively (Figure 2a–c).

Morphology and composition of the consortia envelope at the nanoscale. A combination of cell localization with FITC staining and SEM observations revealed the structures of the ANME-2-SRB consortia, which were found to be completely covered with laminated and cementing materials (Figure 3a–b). The EDS analysis of the lamina substance showed a high abundance of Si, Al, and O, indicating a mineral composition similar to that of phyllosilicate (Figure 3c); the cementing material similarly contained high levels of O and Si, and low abundances of Al, Mg, Ca, Fe, and Na (Figure 3d). Selected area electron diffraction by transmission electron microscopy on the poorly crystallized and laminated siliceous materials yielded similar structures consistent with kaolinite (Supplementary Figure S4). A notable peak of carbon was detected from both the laminated and cementing materials, which could have been derived from the exopolymeric substance.

Silicon was found distributed around the whole cell consortia, as mapped by NanoSIMS (Figure 4a), and was also distributed at the interface between the two dividing parts of the consortia (Figure 4c–d). The ratio of Si to Al varied within a range of approximately 1–4 (Figure 4b). Again, a similar distribution of silicon was observed in all of the consortia of the enriched cell cultures (Figure 4e–f), indicating active silicon mineralization.

To test whether the consortia envelope contained carbonates, we used $^{12}C^{14}N$ and ^{31}P ion mapping to localize the cellular components, and ^{12}C ion mapping to delineate the distribution of the entire carbon element, including carbonate. As shown in Figure 5, the patterns of the $^{12}C^{14}N$ and ^{31}P mappings were almost identical to those of the ^{12}C ion mapping on all of the analyzed layers (Figure 5d–f), indicating the absence of carbonates around the microbial consortia. The wrinkled edge of the $^{12}C^{14}N$ and ^{31}P patterns may represent carbon from extracellular polymers, which shrunk when the sample was dried during sample treatment (Figure 5d–f).

Cell envelope serving as the adhering matrix. The siliceous structure may have provided a surface for additional microbial adhesive growth, which is one of the most important survival strategies used by all microorganisms[21]. Surface adhesion allows the anchoring of microorganisms in nutritionally advantageous environments. The adhesive growth of Betaproteobacteria observed on the surface of the AOM consortia accounted for approximately 1% of the whole consortia (Figure 6a–b). Occasionally, microorganisms of unknown types were observed to attach to the surface of the consortia envelope (e.g., Figure 6c). In this way, the clay mineral envelope served as an active interface for the adhesive growth of extra-consortia microorganisms. This would explain the observations from previous magnetic bead capture experiments showing that other types of microorganisms can form cell aggregates in combination with ANME-SRB[8]. Moreover, associated substrate exchange may occur
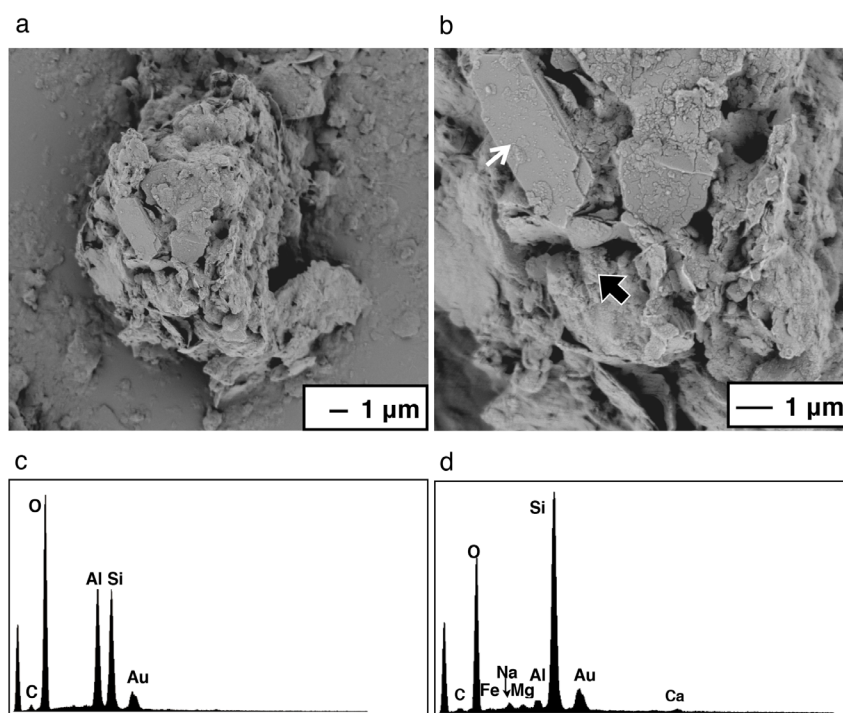

Figure 3 | **SEM and EDS analyses of AOM consortia.** (a) SEM image of the entire consortia. (b) Magnification of an area in (a). (c) EDS analysis of the mineral structure of a representative lamina (white arrow). (d) Analysis of a typical cementing mineral (arrow).
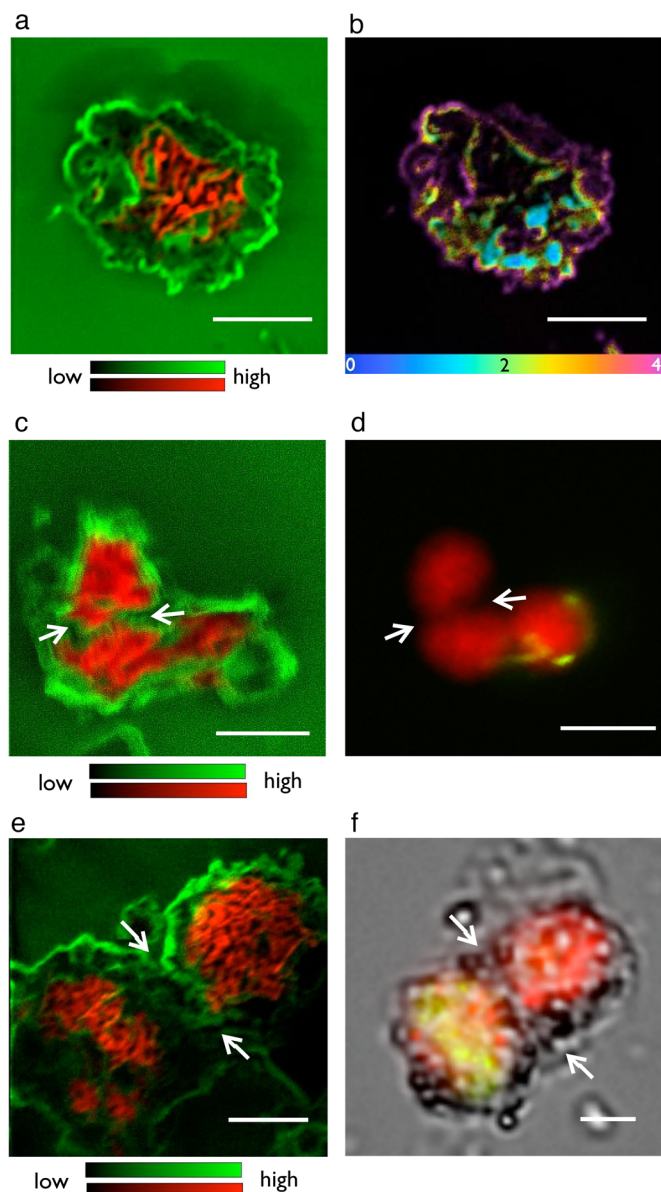
Figure 4 | NanoSIMS mapping and the corresponding FISH imaging of representative AOM consortia from a stored sedimentary marine sample (a–d) and enriched culture (e–f). (a) Overlays of $^{12}C^{14}N$ (red) and ^{28}Si (green) ion images of a consortium. (b) The Si/Al ratio image of the same consortium with Hue-Saturation-Intensity, in which the Si/Al ratios of ≥ 4 are in purple. (c, e) The $^{12}C^{14}N$ (red) and ^{28}Si (green) ion distribution of a fissuring consortium (c). (d, f) The corresponding FISH micrograph of the same consortia in the stored marine sedimentary sample (c) and enriched sample (f), respectively. In (c–f), the arrows indicate the interface of the dividing consortium. In (a, c, d), the green background was made by the glass slide base, $^{12}C^{14}N$ was obtained to localize the cellular components, and the color intensity scales represent the ion-counting numbers in NanoSIMS analysis. The scale bars represent 5 μm.

via the envelope structure because clay minerals have adsorption and exchange properties with respect to dissolved components[22,23].

Discussion

The formation of a siliceous envelope is a bacteria-induced mineralization of clay that has been found to be a common eco-physiological process[24]. Clay-encrusted bacteria have been identified from varied geochemical environments, such as the sediment of iron-rich rivers or lakes and geothermal environments[24,25]. Generally clayey minerals can be formed via three pathways: $Si(OH)_4$ interacts with positively charged $R–NH_3^+$ groups on the cell surface and induces silica to nucleate and grow[26], dissolved silicate and aluminum species adhere indirectly to negatively charged $COOH^-$ or PO_4^{3-} groups on the cell wall and associated exopolymer via a metal cation bridge[24], or colloidal species of (Fe, Al)-silicate react directly with either cellular polymers or adsorbed iron that eventually transform into clay minerals[24].

It has been reported that the physiological activity of cyanobacteria can shift the local pH from 3.4 to 9 (or higher) to induce the dissolution of quartz[27]. AOM consortia may similarly cause a release of silicon from the solid phase. Silica has high solubility and dissolution rates in alkaline solutions. In water with a neutral pH, amorphous and crystalline SiO_2 converts to $Si(OH)_4$ following a slow hydrolysis step that produces hydroxyl ions to stimulate the polarization and break-up of the Si-O[28]. In cold seep environment, HCO_3^- and HS^- produced from AOM cause an increase in alkalinity. Experimentally, ANME and associated bacteria in a high-pressure continuous bioreactor resulted in an increase of pH from 7.0 to 8.5 after 40 days incubation[29]. A recent study on silicification in seeps suggested that the increase in pH resulting from AOM was the main factor for the dissolution of diatom silica skeletons[30]. However, high-resolution *in situ* measurements of pH in sediment with high AOM activity showed that the pH value varied between 7.7 and 7.9, which is a typical pH range for marine sediment[31]. It is possible that the pH increase resulting from the eco-physiological activity of AOM is compensated by protons released during silica dissolution and carbonate precipitation. We suggest that AOM may accelerate the process of silica leaching and that the free silica will redeposit on the surface of the AOM consortia via any of the above-mentioned pathways. The absence of carbonate minerals on the surface of AOM consortia suggests that the microenvironment of the consortia is not favorable for the precipitation of carbonate. Organic components secreted by microorganisms either favor or inhibit the precipitation of carbonate, depending on their intrinsic characteristics[20,32]; however, this inhibition does not affect carbonate precipitation elsewhere in the bulk system.

We compared a stored marine sediment sample and an AOM enrichment culture to exclude potential bias resulting from laboratory manipulations. The same extracellular structures were identified in all of the AOM consortia, which strongly suggests active biomineralization mediated by AOM consortia. This AOM-mediated biomineralization is summarized in the model shown in Figure 7. AOM metabolism increases the alkalinity of the microenvironment, accelerating the leaching and dissolution of silica, which re-deposits on the surface of the consortia by biological adsorption. The primary poorly crystallized silica gradually ages to more stable crystalline phases over time. The precipitation of carbonates on the surface of the consortia is, however, prohibited due to the high solubility product values of carbonates when compared with those of clay minerals.

The development of a siliceous envelope may benefit the microbial consortia in at least three aspects. First, it will enhance the structural integrity of the syntrophic members. The association between ANME and SRB is thought to be the result of an ancient type of multicellular symbiosis[33]. AOM consortia grow by increasing the cell numbers and size of the consortia, and larger consortia may eventually break into two or more aggregates[19]. Second, as enclosure by the siliceous envelope may keep ANME and SRB together, it has also been suggested that clay-like minerals may provide a source of exchangeable nutrients[22]. Experimental studies have demonstrated that clays, such as montmorillonite and kaolinite, can host methane hydrate[34,35]. Finally, it would be very interesting to test in the future whether the clay envelope surrounding the AOM cell consortia is capable of methane storage, thus serving as a cell-adhering material and an exchangeable matrix of nutrients, as described above.
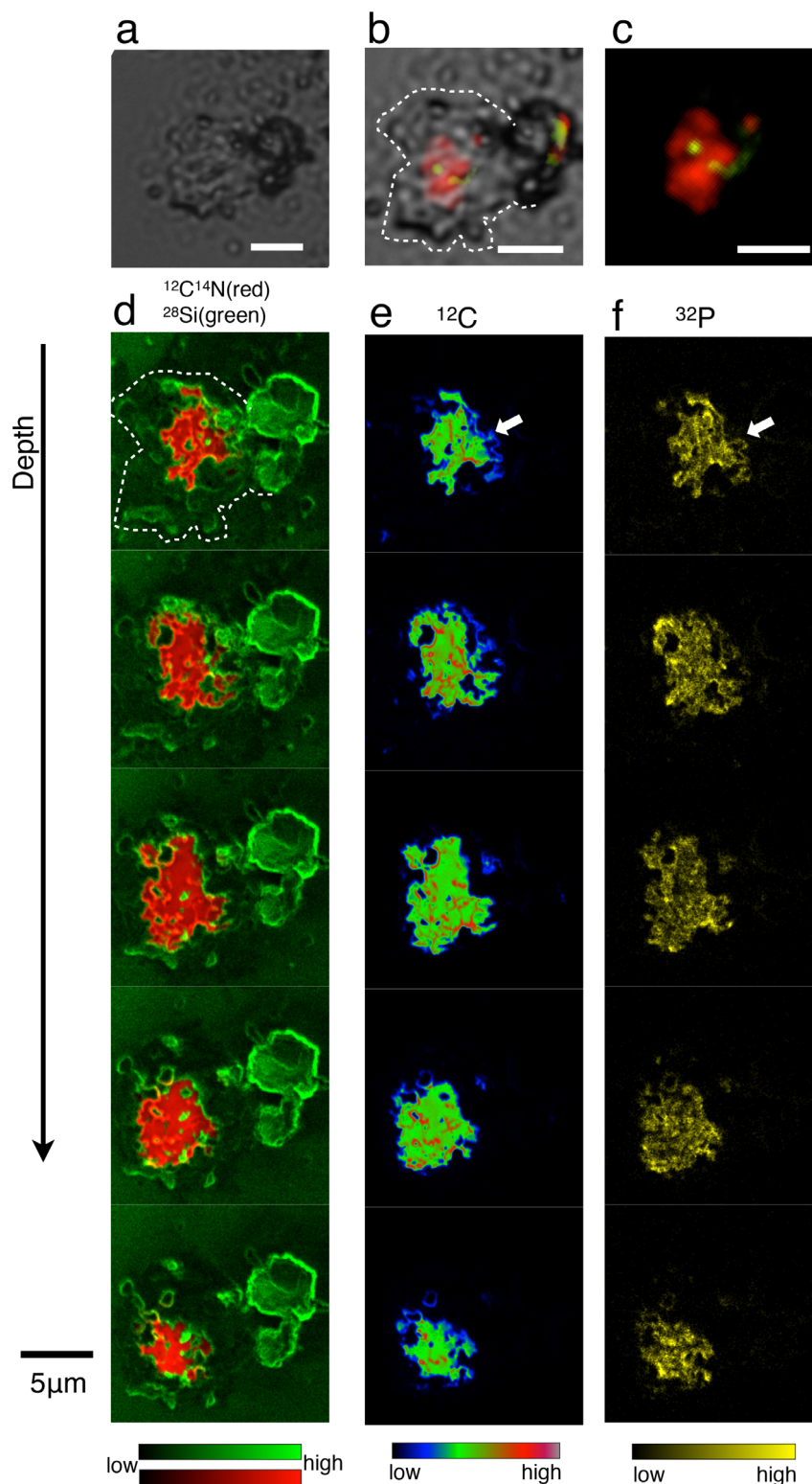
Figure 5 | Micrographs and serial top-down ion distribution of a representative ANME-2/SRB consortium from a stored marine sedimentary sample. (a) Bright-field photomicrographs of the consortium. (b) Overlay of (a) and (c). (c) Epifluorescent FISH image of a microbial consortium, with the ANME in red and the SRB in green. (d) Serial overlays of $^{12}C^{14}N$ (red) and ^{28}Si (green) ion distributions of the consortium, which were acquired to locate the cellular components and siliceous minerals. The green background was caused by the glass slide. (e) Serial images of ^{12}C (in Hue-Saturation-Intensity) ion distribution, which were acquired to localize potential carbonates around the consortium. (f) ^{31}P (yellow) ion images, which were acquired to locate the cellular biomass such as nucleic acids and protein. For columns (d–f), the color intensity scales represent the ion counts in the NanoSIMS analysis. The bars represent 5 μm in all cases. The dashed lines in (b) and (d) indicate the margin of the consortia envelope. In (e) and (f), the wrinkled edges (arrows) were assigned to polysaccharide and protein within the extracellular organic matrix, which shrank during the sample preparation for NanoSIMS.
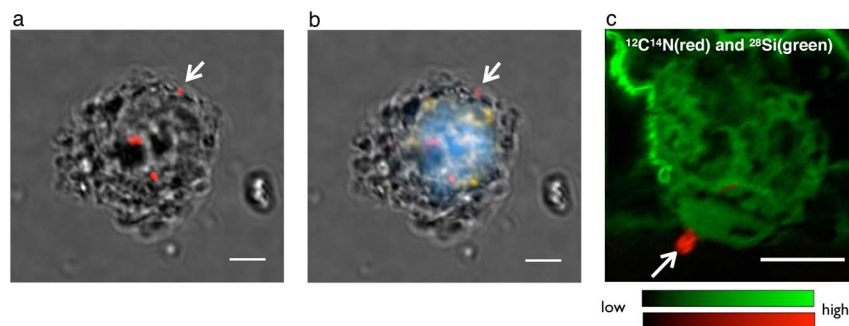
Figure 6 | Micrographs of ANME and associated bacteria. (a, b) Overlays of a representative consortium from a stored sedimentary marine sample consisting of ANME-2 (blue), SRB (yellow), and Betaproteobacteria (red). The arrow indicates a typical Betaproteobacteria cell adhering to the siliceous envelope. (c) Overlay of $^{12}C^{14}N$ (red) and ^{28}Si (green) ion images of a consortium envelope surface, to which an unknown microorganism (arrow) was attached. The color intensity scales in (c) represent the ion-counting numbers in the NanoSIMS analysis. The scale bars represent 5 μm.

The discovery of AOM consortia encrusted with clayey minerals also reveals a mechanism involved in the preservation and fossilization of AOM in modern and ancient marine sediments. AOM consortia in hydrocarbon seeps are common in the sediments[1,14] where methane-derived ^{13}C-depleted carbonate precipitates[36]. However, no direct fossilization of AOM cells has been discovered yet. Recent studies on the microstructures in methane seep carbonates interpreted these bacteriomorphs to be pseudofossils resulting from the diagenetic alteration of euhedral Fe-sulfide framboids[37]. On the basis of that work, we argue that microstructures with a particular Si-Al composition in cold-seep ^{13}C-depleted carbonates may be fossilized AOM consortia. This mechanism of mineralization could be used in searching for fossilized AOM in diagenetic marine carbonaceous sediments or ancient marine sedimentary rocks. Considering that AOM may have represented an important biological process in the ancient anoxic biosphere, this siliceous structure may have played historically significant roles in the oceanic silicon cycle and AOM burial, similar to that played by the siliceous cell walls of diatoms and cyanobacteria in modern oceans.

Methods

Sample description. The sample used in this study had a sediment depth of 0–40 cm and was originally collected in 2006 from the Capt Aryutinov Mud Volcano (N35°39.700″ W07°20.012″) in the Gulf of Cadiz, Atlantic Ocean, 1200 m below sea level)[29]. The collected sediment was stored at ambient pressure in an artificial seawater medium (see reference 29) at 4°C that was supplemented with methane.

Anaerobic oxidation of methane coupled to a sulfate reduction (SR-AOM) activity of 0.29 μmol sulfide production/gdw/day was measured using the methods described previously[29].

The enriched ANME-2-SRB culture was obtained from a high-pressure (8 MPa) continuous bioreactor for AOM enrichment, where a high SR-AOM activity of 9.22 μmol sulfide production/gdw/day was obtained as described previously[29]. Within the enrichment, 99% of the biomass was from AOM consortia, in which ANME-2 and SRB were found to be increased by 12.5 and 8.4 fold, respectively[38].

FISH. Sample fixation and FISH procedures followed previously described methods[39]. Samples were fixed for 12 hours with 2% formaldehyde, washed twice with PBS, and finally re-suspended with a 1 : 1 mix of PBS/ethanol. Fixed samples were filtered through a polycarbonate membrane with a 0.22 μm pore size (Millipore, Eschborn, Germany). Then, the membrane was subjected to hybridization and washing procedures as described previously[39]. Probes specific to ANME-2 (ANME-2-538-Alexa594 and ANME-2-538-AMCA)[40], *Desulfobacteriaceae* (DSS658-Alexa488)[41], and Betaproteobacteria (BET-42a-Alexa594)[42] were purchased from Life Technologies (Shanghai, China). For FISH with multiple probes, a formamide concentration of 50% was used for both DSS658 and ANME-2-538, and of 35% for BET-42a.

FITC and Alcian Blue staining procedures. For protein staining, samples were first centrifuged at $9000 \times g$ for 1 min to remove the supernatant. The precipitate was then incubated with fluorescein isothiocyanate (FITC; Sigma-Aldrich, St. Louis, MO, USA) solution (0.5 g/L distilled water) for 30 minutes at room temperature followed by triple washing with 18 MΩ deionized distilled water. The procedures for Alcian Blue staining were conducted as described previously[43].

Light microscopy. The AOM consortia were observed with an Eclipse 90i automated microscope system (Nikon, Tokyo, Japan). Monochrome images were taken using a CoolSNAP HQ2 camera (Photometrics, Tucson, AZ, USA) and color images were
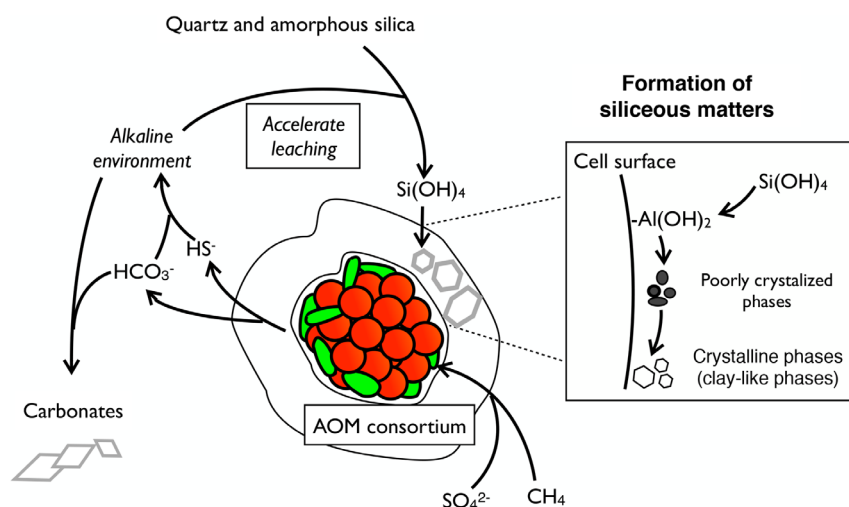

Figure 7 | Model for the ANME/SRB-mediated precipitation of carbonate and clay minerals. The AOM consortia perform anaerobic oxidation of methane with sulfate reduction generating HCO_3^- and HS^- as products, which increase the alkalinity of the microenvironment. Consequently, the precipitation of carbonate minerals and the dissolution of silica are stimulated. The dissolved silica in the form of $Si(OH)_4$, which is initially amorphous and may eventually crystallize upon aging, will re-deposit on the surface of the microbial consortia due to microbial adsorption.

taken with a PowerShot G11 camera (Canon, Tokyo, Japan). The images were processed with NIS Element Ar image software (Nikon).

FISH-NanoSIMS. NanoSIMS analysis was conducted on a NanoSIMS 50L (CAMECA, Gennevilliers Cedex, France) at the Institute of Geology and Geophysics, Chinese Academy of Sciences (Beijing), and the ion images were processed with ImageJ software[44]. The NanoSIMS samples were examined on a round glass (1 inch in diameter). The FISH-stained samples were washed from the polycarbonate membrane with 18 MΩ deionized distilled water and a 0.5 μl sample was dropped onto the round glass. Then, the sample drops were dried at room temperature, which led to the formation of spots on the round glass. As dried microbial consortia display irregular patterns of FISH signals, the spots on the glass were mounted with 0.1 μl 18 MΩ deionized distilled water and micrographs were quickly obtained before the samples dried again. Micrographs of consortia at high magnification were taken for identification of the microbial consortia and lower magnification images covering the whole sample spot were taken for localization (e.g., Supplementary Figure S5). These micrographs were used as maps to locate the consortia under NanoSIMS. Finally, the round glasses were sputter-coated with gold (25–90 s at 30 mA) and used for NanoSIMS analysis.

SEM and EDS. Observations by SEM and EDS analyses were conducted with a NOVA NanoSEM 230 (FEI, Shanghai, China) and AZTec X-Max80 EDS (Oxford Instruments, Abingdon, UK), respectively. Samples stained with FITC were deposited on 0.3×0.3 mm^2 glass squares, which were clipped from cover glasses (Thermo Fisher Scientific, Waltham, MA, USA). Cell localization and gold coating followed the same procedures described above.

1. Knittel, K. & Boetius, A. Anaerobic oxidation of methane: progress with an unknown process. *Annu. Rev. Microbiol.* **63**, 311–334 (2009).
2. Hinrichs, K.-U., Hayes, J. M., Sylva, S. P., Brewer, P. G. & DeLong, E. F. Methane-consuming archaebacteria in marine sediments. *Nature* **398**, 802–805 (1999).
3. Boetius, A. *et al.* A marine microbial consortium apparently mediating anaerobic oxidation of methane. *Nature* **407**, 623–626 (2000).
4. Orphan, V. J., House, C. H., Hinrichs, K.-U., McKeegan, K. D. & DeLong, E. F. Multiple archaeal groups mediate methane oxidation in anoxic cold seep sediments. *Proc. Natl. Acad. Sci. USA* **99**, 7663–7668 (2002).
5. Knittel, K., Lösekann, T., Boetius, A., Kort, R. & Amann, R. Diversity and distribution of methanotrophic archaea at cold seeps. *Appl. Environ. Microbiol.* **71**, 467–479 (2005).
6. Niemann, H. *et al.* Novel microbial communities of the Haakon Mosby mud volcano and their role as a methane sink. *Nature* **443**, 854–858 (2006).
7. Schreiber, L., Holler, T., Knittel, K., Meyerdierks, A. & Amann, R. Identification of the dominant sulfate-reducing bacterial partner of anaerobic methanotrophs of the ANME-2 clade. *Environ. Microbiol.* **12**, 2327–2340 (2010).
8. Pernthaler, A. *et al.* Diverse syntrophic partnerships from deep-sea methane vents revealed by direct cell capture and metagenomics. *Proc. Natl. Acad. Sci. USA* **105**, 7052–7057 (2008).
9. Grossman, E. L., Cifuentes, L. A. & Cozzarelli, I. M. Anaerobic methane oxidation in a landfill-leachate plume. *Environ. Sci. Technol.* **36**, 2436–2442 (2002).
10. Holler, T. *et al.* Thermophilic anaerobic oxidation of methane by marine microbial consortia. *ISME J.* **5**, 1946–1956 (2011).
11. Durisch-Kaiser, E., Klauser, L., Wehrli, B. & Schubert, C. Evidence of intense archaeal and bacterial methanotrophic activity in the Black Sea water column. *Appl. Environ. Microbiol.* **71**, 8099–8106 (2005).
12. Eller, G., Känel, L. & Krüger, M. Cooccurrence of aerobic and anaerobic methane oxidation in the water column of Lake Plußsee. *Appl. Environ. Microbiol.* **71**, 8925–8928 (2005).
13. Alain, K. *et al.* Microbiological investigation of methane- and hydrocarbon-discharging mud volcanoes in the Carpathian Mountains, Romania. *Environ. Microbiol.* **8**, 574–590 (2006).
14. Boetius, A. *et al.* A marine microbial consortium apparently mediating anaerobic oxidation of methane. *Nature* **407**, 623–626 (2000).
15. Wegener, G., Niemann, H., Elvert, M., Hinrichs, K. U. & Boetius, A. Assimilation of methane and inorganic carbon by microbial communities mediating the anaerobic oxidation of methane. *Environ. Microbiol.* **10**, 2287–2298 (2008).
16. Michaelis, W. *et al.* Microbial reefs in the Black Sea fueled by anaerobic oxidation of methane. *Science* **297**, 1013–1015 (2002).
17. Jørgensen, B. B. & Boetius, A. Feast and famine--microbial life in the deep-sea bed. *Nat. Rev. Microbiol.* **5**, 770–781 (2007).
18. Boetius, A. & Wenzhöfer, F. Seafloor oxygen consumption fuelled by methane from cold seeps. *Nat. Geosci.* **6**, 725–734 (2013).
19. Nauhaus, K., Albrecht, M., Elvert, M., Boetius, A. & Widdel, F. *In vitro* cell growth of marine archaeal-bacterial consortia during anaerobic oxidation of methane with sulfate. *Environ. Microbiol.* **9**, 187–196 (2007).
20. Gadd, G. M. Metals, minerals and microbes: geomicrobiology and bioremediation. *Microbiology* **156**, 609–643 (2010).
21. Dunne, W. M. Bacterial adhesion: seen any good biofilms lately? *Clin. Microbiol. Rev.* **15**, 155–166 (2002).
22. Phoenix, V. R. & Konhauser, K. O. Benefits of bacterial biomineralization. *Geobiology* **6**, 303–308 (2008).
23. Ehrlich, H., Demadis, K. D., Pokrovsky, O. S. & Koutsoukos, P. G. Modern views on desilicification: biosilica and abiotic silica dissolution in natural and artificial environments. *Chem. Rev.* **110**, 4656–4689 (2010).
24. Konhauser, K. O. & Urrutia, M. M. Bacterial clay authigenesis: a common biogeochemical process. *Chem. Geol.* **161**, 399–413 (1999).
25. Ferris, F., Beveridge, T. & Fyfe, W. Iron-silica crystallite nucleation by bacteria in a geothermal sediment. *Nature* **320**, 609–611 (1986).
26. Dekov, V. M. *et al.* Hydrothermal nontronite formation at Eolo seamount (Aeolian volcanic arc, Tyrrhenian Sea). *Chem. Geol.* **245**, 103–119 (2007).
27. Brehm, U., Gorbushina, A. & Mottershead, D. The role of microorganisms and biofilms in the breakdown and dissolution of quartz and glass. *Palaeogeogr. Palaeoclimatol. Palaeoecol.* **219**, 117–129 (2005).
28. Dove, P. M., Han, N., Wallace, A. F. & De Yoreo, J. J. Kinetics of amorphous silica dissolution and the paradox of the silica polymorphs. *Proc. Natl. Acad. Sci. USA* **105**, 9903–9908 (2008).
29. Zhang, Y., Henriet, J.-P., Bursens, J. & Boon, N. Stimulation of *in vitro* anaerobic oxidation of methane rate in a continuous high-pressure bioreactor. *Bioresour. Technol.* **101**, 3132–3138 (2010).
30. Kuechler, R. R. *et al.* Miocene methane-derived carbonates from southwestern Washington, USA and a model for silicification at seeps. *Lethaia* **45**, 259–273 (2012).
31. de Beer, D. *et al. In situ* fluxes and zonation of microbial activity in surface sediments of the Håkon Mosby Mud Volcano. *Limnol. Oceanogr.* **51**, 1315–1331 (2006).
32. Kawano, M. & Hwang, J. Roles of microbial acidic polysaccharides in precipitation rate and polymorph of calcium carbonate minerals. *Appl. Clay Sci.* **51**, 484–490 (2011).
33. Bonner, J. T. The origins of multicellularity. *Integr. Biol.* **1**, 27–36 (1998).
34. Cygan, R. T., Guggenheim, S. & Koster van Groos, A. F. Molecular models for the intercalation of methane hydrate complexes in montmorillonite clay. *J. Phys. Chem. B* **108**, 15141–15149 (2004).
35. Liu, D. *et al.* High-pressure adsorption of methane on montmorillonite, kaolinite and illite. *Appl. Clay Sci.* **85**, 25–30 (2013).
36. Jiang, G., Kennedy, M. J. & Christie-Blick, N. Stable isotopic evidence for methane seeps in Neoproterozoic postglacial cap carbonates. *Nature* **426**, 822–826 (2003).
37. Bailey, J. V. *et al.* Pseudofossils in relict methane seep carbonates resemble endemic microbial consortia. *Palaeogeogr. Palaeoclimatol. Palaeoecol.* **285**, 131–142 (2010).
38. Zhang, Y., Maignien, L., Zhao, X., Wang, F. & Boon, N. Enrichment of a microbial community performing anaerobic oxidation of methane in a continuous high-pressure bioreactor. *BMC Microbiol.* **11**, 3132–3138 (2011).
39. Pernthaler, J., Glöckner, F.-O., Schönhuber, W. & Amann, R. Fluorescence *in situ* hybridization with rRNA-targeted oligonucleotide probes. *Meth. Microbiol.* **30**, 207–226 (2001).
40. Treude, T., Knittel, K., Blumenberg, M., Seifert, R. & Boetius, A. Subsurface microbial methanotrophic mats in the Black Sea. *Appl. Environ. Microbiol.* **71**, 6375–6378 (2005).
41. Manz, W., Eisenbrecher, M., Neu, T. R. & Szewzyk, U. Abundance and spatial organization of Gram-negative sulfate-reducing bacteria in activated sludge investigated by *in situ* probing with specific 16S rRNA targeted oligonucleotides. *FEMS Microbiol. Ecol.* **25**, 43–61 (1998).
42. Manz, W., Amann, R., Ludwig, W., Wagner, M. & Schleifer, K.-H. Phylogenetic oligodeoxynucleotide probes for the major subclasses of proteobacteria: problems and solutions. *Syst. Appl. Microbiol.* **15**, 593–600 (1992).
43. Bosak, S. *et al.* A novel type of colony formation in marine planktonic diatoms revealed by atomic force microscopy. *PLoS One* **7**, e44851 (2012).
44. Schneider, C. A., Rasband, W. S. & Eliceiri, K. W. NIH Image to ImageJ: 25 years of image analysis. *Nat. Methods* **9**, 671–675 (2012).

Acknowledgments

Author contributions

Y.C., F.W., Y.L. and X.X. conceived and designed the experiments. Y.C., Y.L. and H.L. performed the experiments. Y.C., Y.L. and F.W. wrote the manuscript text, and Y.C., F.W., Y.L., G.Z., Y.L. and X.X. analyzed the data. Y.C. prepared Figures 1–5 and Supplementary Figure S5, HL prepared Supplementary Figures S1–3, and Y.L. prepared Supplementary Figure S4. All of the authors reviewed and approved the manuscript.

Additional information